Published in final edited form as:
Biosens Bioelectron. 2010 September 15; 26(1): 182–188. doi:10.1016/j.bios.2010.06.007.

Flow-through immunosensors using antibody-immobilized polymer monoliths

Jikun Liu[a], **Chien-Fu Chen**[a], **Chih-Wei Chang**[a], and **Don L. DeVoe**[a,*]
[a]Department of Mechanical Engineering, University of Maryland, College Park, MD 20742, USA

Abstract

High-sensitivity and rapid flow-through immunosensors based on photopolymerized surface-reactive polymer monoliths are investigated. The porous monoliths were synthesized within silica capillaries from glycidyl methacrylate and ethoxylated trimethylolpropane triacrylate precursors, providing a tortuous pore structure with high surface area for the immobilization of antibodies or other biosensing ligands. The unique morphology of the monolith ensures efficient mass transport and interactions between solvated analyte molecules and covalently immobilize antibodies anchored to the monolith surface, resulting in rapid immunorecognition. The efficacy of this approach is demonstrated through a direct immunoassay model using anti-IgG as a monolith-bound capture antibody and fluorescein-labeled IgG as an antigen. *In situ* antigen measurements exhibited a linear response over a concentration range between 0.1 - 50 ng/mL with 5 min assay times, while controllable injection of 1 μL volumes of antigen through the monolith elements yielded a mass detection limit of 100 pg (~700 amol). These results suggest that porous monolith supports represent a flexible and promising material for the fabrication of rapid and sensitive immunosensors suitable for integration into capillary or microfluidic devices.

Keywords

Monolith; Solid support; Biosensor; Immunoassay; Antibody

1. Introduction

Biosensors represent an expansive family of detection systems that utilize biological molecules as sensing elements to probe variations in selected physicochemical properties of analyte molecules (Borisov and Wolfbeis 2008). In comparison to conventional instrumental analysis techniques such as chromatography and spectroscopy, biosensors are generally highly sensitive, selective, compact, and adaptable to on-site or in-field applications. As an important subset of affinity biosensors, immunosensors exploit non-covalent antibody-antigen interactions to detect and quantify target analytes. Due to the unique recognition process and strong affinity of antibody-antigen interactions, immunosensors are highly selective and sensitive, and capable of identifying low abundance species from complex sample matrixes in competitive and noncompetitive assays. In a competitive assay, the

*Corresponding author. Current address: 3139 Glenn L. Martin Hall, Department of Mechanical Engineering, University of Maryland, College Park, MD 20742, USA, Tel.: +1 301 405 8125, ddev@umd.edu .

sample is mixed with a labeled form of the antigen of interest, resulting in a signal intensity is inversely proportional to the concentration of the unlabeled antigen within the sample. In a noncompetitive assay, unbound sample components are removed from the antibody capture surface after establishing antibody-antigen interactions, followed by quantification of the bound antigen. In a direct immunoassay, captured antigen is measured directly. e.g. by prelabeling the antigen with a fluorescent probe. In contrast, sandwich assays employ antigens with at least two epitopes which can bind to the capture antibodies immobilized on the immunosensor surface as well as a labeled secondary antibody for enhanced specificity and signal amplification (Bange et al. 2005; Borisov and Wolfbeis 2008). Immunosensors based on these various formats have been widely employed to detect toxins (Ionescu et al. 2004; Konry et al. 2003; Parker et al. 2009), explosives (Bakaltcheva et al. 1999; Van Bergen et al. 2000), pesticides (Kim et al. 2006; Szekacs et al. 2003; Valera et al. 2007), drugs (Anderson and Miller 1988; Benito-Pena et al. 2005), proteins (Alvarez et al. 2009; Lepesheva et al. 2000), cancer markers (Dai et al. 2003; Munge et al. 2009; Yu et al. 2006), virus (Heinze et al. 2009; Ionescu et al. 2007; Konry et al. 2005; Zuo et al. 2004) and bacteria (Bae et al. 2004; Wang et al. 2008; Yang et al. 2004).

Regardless of the assay type, immobilization of antibodies on a solid support is a key requirement for all immunoassays. In a traditional immunoassay, primary antibodies are adsorbed onto the polymer surfaces of titer plate wells. Alternately, using materials including glass, silicon, quartz, polymers and metals that allow anchoring of antibodies through appropriate surface modifications, a variety of alternative antibody support topologies have been developed, including planar films (Kurita et al. 2006; Rowe et al. 1999; Sai et al. 2006), porous membranes (Tang et al. 2008), optical fibers (McCormack et al. 1997; Narang et al. 1997), nanowires (Bangar et al. 2009; Wang et al. 2008) and microbeads (Biagini et al. 2004; Heinze et al. 2009; Matsunaga et al. 2007). Of particular interest are flow-through immunosensor designs, in which sample is hydrodynamically driven past one or more sites with immobilized primary antibodies. Flow-through devices comprising an open flow path with antibodies bound to the sidewalls have been reported using both silica capillaries (Mastichiadis et al. 2002; Narang et al. 1998) and microfluidic channels (Dong et al. 2007; Gervais and Delamarche 2009). While flow-through designs can enhance antigen-antibody interactions by increasing mass transport due to the superposition of convective flow on top of simple diffusion, open-flow systems retain the same basic topology as simple planar sensor surfaces, with probe density limited by the two-dimensional nature of the capture surface. One approach to improving the density of primary antibodies within the detection volume is to employ a porous anchoring medium in the flow path. Various porous media have been explored for this purpose in large-scale flow-through systems, including agarose gel (Gonzalez-Martinez et al. 1997) and polymer frits or membranes (Abdel-Hamid et al. 1999; Alvarez et al. 2009; Charles et al. 2000; Jain et al. 2004). These porous materials provide larger surface areas than planar supports for the immobilization of capture species, thereby increasing detection sensitivity, while also providing smaller characteristic diffusion times for antigens or secondary antibodies infused through the micron-scale pores. However, seamless integration of suitable porous media into capillary or microfluidic immunoassays remains a challenge. For example, while packed microbeads have been used to anchor antibodies inside microfluidic channels (Kim et al. 2009), weirs or frits are required to retain packed the beads within the flow path, and defining discrete sensing regions within complex microchannel networks is challenging.

Here we propose an alternative solid support for microscale flow-through immunoassays based on polymer monoliths. Monoliths are highly porous inorganic or organic materials (Svec and Huber 2006) commonly used as chromatographic stationary phases (Guiochon 2007) and solid-phase extraction elements (Yu et al. 2001) for analytical separation, sample processing and purification. More recently, monoliths have been applied to a range of

microfluidic systems including proteolytic bioreactors (Peterson et al. 2002), mixers (Rohr et al. 2001), valves (Chen et al. 2008) and electrospray emitters (Koerner et al. 2004). Monolith preparation is achieved by a range of polymerization techniques, with free radical polymerization the most commonly used method. Both heat and UV radiation can initiate the polymerization process, with the latter approach suitable for fabrication of monoliths with well defined geometries at specific locations. Monoliths with different porosity, surface area and flow resistance may be synthesized by tuning relative concentrations of monomers, organic solvents and free radical initiator. By incorporating monomers with desired functionalities in the polymerization, reactive moieties are introduced to the monolith surface, thus facilitating covalent immobilization of antibodies and enzymes to the surface. This method has been employed in applications including preparative proteolytic bioreactors (Peterson et al. 2002) and affinity chromatography (Mallik and Hage 2006) where the digestion of samples and capture of target analytes are performed in monoliths and the products are monitored with downstream detectors in releasing processes. Although originally developed for large-scale sample preparation, the fabrication techniques and surface chemistries of surface-reactive monoliths can be directly adapted to the development of microscale immunosensors.

To demonstrate the utility of monoliths as porous supports for immunoassays, *in situ* photopolymerized epoxide polymethacrylate monoliths have been fabricated within silica capillaries. A multi-step reaction process involving thiol treatment and succinimidyl ester grafting was utilized to activate the monolith, followed by the covalent immobilization of antibodies. The performance of the system was verified through a direct immunoassay test, using mouse IgG as a capture antibody and fluorescein-labeled anti-mounse IgG as a target antigen. Our initial results reveal that monoliths can serve as a novel and effective solid support for the development of rapid, sensitive, versatile immunosensors. The fabrication process is also suitable for further integration of monolithic immunosensor elements into disposable micro total analysis systems.

2. Experiment Section

2.1 Materials

Glycidyl methacrylate (GMA), cyclohexanol, 2,2′-dimethoxy-2-phenylacetophenone (DMPA), sodium chloride, potassium chloride, sodium phosphate monobasic, sodium phosphate dibasic, hydrochloric acid (HCl), trimethoxysilylpropyl methacryalte (TPM), N-γ-maleimidobutyryloxy succinimide ester (GMBS), bovine serum albumin (BSA), fluorescein isothiocyanate (FITC)-labeled rabbit IgG (MW~140 kDa) were purchased from Sigma-Aldrich (St. Louis, MO). Goat anti-rabbit IgG, HPLC water, dimethylformamide (DMF), methanol, ethanol and acetone was obtained from Thermo Fisher Scientific (Rockford, IL). Ethoxylated trimethylolpropane triacrylate (SR454) was received as a free sample from Sartomer (Warrington, PA). Polyimide coated silica capillary with 360 μm O.D. and 100 μm I.D. was procured from Polymicro (Phoenix, AZ).

2.2 Monolith preparation

Before monolith preparation, the silica capillary inner surface was treated with TPM for anchoring the monolith. Briefly, two sets of MicroTight fittings and unions (Upchurch Scientific, Oak Harbor, WA) were connected to both ends of a 50 cm long capillary. Acetone, HPLC water, and 0.1 M HCl were then injected using a syringe connected to one of the unions to rinse the capillary. After rinsing, the two unions were capped with gauge plugs (Upchurch Scientific) to seal 0.1 M HCl solution in the capillary, and then the capillary assembly was kept in an oven set at 105 °C for at least 12 h to condition the capillary surface. The conditioned capillary was cooled to room temperature and its polymer

coating removed with a lighter. After displacing the HCl solution with HPLC water, a 30% (v/v) TPM ethanol solution was filled in the capillary. Silanization of the capillary surface was allowed to proceed in dark for 24 h. The TPM treated capillary was rinsed with absolute ethanol and dried with nitrogen before use.

To synthesize a monolith section, first, a pre-monolith solution containing 24% (w/w) GMA, 16% (w/w) SR454, 50% (w/w) cyclohexanol, and 10% (w/w) methanol was prepared. Photoinitiator (DMPA) was added to the pre-monolith solution at 1% (w/w) of the combined weight of GMA and SR454. After filled with the pre-monolith, the outer surface of the capillary was coated with an opaque liquid rubber coating (Plasti Dip International, Blaine, MN) except for a 3 mm long section. The masked capillary was exposed to a UV source (PRX-1000; Tamarack Scientific, Corona, CA) with an incident power of 22.0 mW/cm^2 for 360 s, forming a monolith segment within the exposed capillary region. The monolith section was thoroughly rinsed with absolute methanol then 20% (v/v) methanol aqueous solution before further treatment.

2.3 Antibody Immobilization

The surface of the GMA-SR454 monolith was modified through a multi-step reaction process. In the first step, a fresh 2 M sodium hydrosulfide solution was prepared by dissolving the compound in a methanol-0.1 M aqueous sodium phosphate dibasic mixture (20:80, v/v). Before use, the pH of the solution was adjusted to about 8.15 using 2 M phosphoric acid solution. The buffered sodium hydrosulfide solution was then infused through the monolith section at 0.5 μL/min for at least 2 h using a PHD-2000 syringe pump (Harvard Apparatus, Holliston, MA) to transform the epoxide groups to thiol groups, followed by a thorough rinsing with 20% (v/v) methanol aqueous solution. To hydrolyze the residual epoxide groups, the thiol grafted monolith was filled with 0.5 M sulfuric acid and kept at 65 °C overnight. After hydrolysis, the monolith was conditioned with HPLC water and ethanol. GMBS solution was prepared by dissolving the powder in a small amount of DMF and diluting with absolute ethanol to a final concentration of 2 mM, and then infused through the monolith at 0.5 μL/min for 1 h. Following the grafting reaction, 1X phosphate buffered saline (PBS, pH 7.4) solution was used to thoroughly rinse the monolith. Goat anti-rabbit IgG (antibody) was diluted in 1X PBS solution to a concentration of 50 μg/mL and pumped through the monolith at 1 μL/min for 1 h. Immediately prior to testing, a solution of 2 mg/mL BSA in 1X PBS was infused through the antibody-immobilized monolith.

2.4 Characterization of antibody-antigen interactions

FITC-labeled rabbit IgG (antigen) solutions with concentrations ascending from 10 to 10000 ng/mL were prepared using 1X PBS solution. BSA was dissolved in all antigen solutions to a concentration of 2 mg/mL to depress possible nonspecific adsorption of antigen to the monolith surface.

To determine the concentration detection limit of the monolith immunosensor, 10 μL volumes of antigen solutions at varying antigen concentrations (0.1, 1, 10, and 50 ng/mL) were continuously loaded through the monoliths at a flow rate of 2 μL/min for 5 min, followed by rinsing of the monolith with 1X PBS. To evaluate the molar detection limit of the sensor, 1 μL volumes of antigen solutions were pumped into the monoliths at a flow rate of 1 μL/min for 1 min using a syringe pump and incubated at room temperature for 10 min. Before fluorescence measurements the monoliths were quickly rinsed with 1X PBS. The background fluorescence intensity of the monolith sections was acquired before all tests and subtracted from the signals in data processing.

A TE-2000 S inverted epi-fluorescence microscope (Nikon, Melville, NY) equipped with an automated X-Y microscope stage and a CoolSnap HQ2 CCD camera (Roper Scientific, Tucson, AZ) was used for fluorescence measurements. An excitation wavelength within the range of 465-495 nm was selected using a B-2E/C blue filter (Nikon) to detect the captured antigen on monolith. A 10×, 0.30 N.A. objective (Nikon) was used for simultaneous imaging and detection.

Data acquisition was performed with Advanced Element software (Nikon). Briefly, a 100 μm (w) × 60 μm (l) rectangular region of interest (ROI) was defined as a detection window located at the front of the monolith section. The monolith was then shifted along its axis to pass the ROI by moving the microscope stage at an average linear velocity of 0.10 mm/s. Fluorescence intensity data were recorded continuously and normalized by dividing the sum of the intensity by the total pixels in a 100 μm (w) × 1000 (l) μm measuring area starting from the monolith front end.

3. Results and discussion

3.1 Monolith synthesis

While a wide range of monolith materials have the potential to be employed as antibody supports, we chose to investigate acrylic monoliths considering their relatively simple preparation, abundant monomer availability, controllable surface chemistry, and favorable physical properties. In particular, UV photopolymerized acrylic monoliths are explored to allow the use of standard photolithographic techniques for patterning desired monolith geometries. Most acrylic monoliths are composed of a mono-vinyl monomer, a di-vinyl crosslinking reagent, and an inert mixture containing several organic solvents for the formation of a proper porous network (Svec 2004). Unfortunately, using established acrylic monolith recipes, we found that it is difficult to reproducibly prepare continuous and homogeneous monolith regions via UV initiated polymerization, while successfully fabricated monoliths commonly exhibit excessive hydrodynamic flow resistance. By simply replacing the di-vinyl with a tri-vinyl crosslinking reagent, however, monoliths with high flow permeability and continuous structure within UV exposed channel sections can be faithfully obtained (Liu et al. 2009). In the present work, we copolymerized GMA, a monomer with a pendant epoxide group, and SR455, a tri-vinyl crosslinking reagent, to prepare surface reactive monolith sections suitable for antibody immobilization. The morphology of the resulting monolith is depicted in Fig. 1. The structure is composed of fused clusters of nearly spherical microglobules approximately 1 μm in diameter, presenting multiple tortuous flow paths with average pore dimensions around 5 μm and a high surface area for immobilization of capturing species. The irregular shape of the clusters limits the packing density and ensures relatively high permeability. The images also reveal anchoring of the monolith to the TPM-modified capillary wall. During the UV-initiated free radical polymerization, covalent bonds are presumably formed between the TPM vinyl groups and the monomer vinyl groups, allowing the in-situ synthesized monolith to have sufficient mechanical stability to withstand high shear forces generated during a flow-through immunoassay.

3.2 Antibody immobilization

The epoxide group is one of the most versatile chemical functionalities in organic synthesis, and epoxide bearing supports are often used as industrial biocatalyst (Mateo et al. 2002; Mateo et al. 2003), proteolytic enzyme bioreactors (Peterson et al. 2002) and affinity chromatography (Mallik and Hage 2006). To permanently anchor biomacromolecules such as enzymes or antibodies on epoxide-rich surfaces, the three-member rings are opened through various nucleophilic addition reactions. It is possible to directly immobilize proteins

to the modified epoxide supports through the reactions of protein primary amines, thiols or other functionalities with the surface epoxides. However, the reaction rate is relatively low, presumably due to the slow reaction kinetics and large steric hindrance of the bulky proteins (Peterson et al. 2002). Acceleration of protein immobilization can be achieved by elongating the linking arms of the active moieties and replacing epoxides with more active capturing functionalities. This strategy is normally implemented by grafting di-amines to the surface epoxides and then linking di-aldehydes to the free primary amines. Proteins are immobilized through reaction between their primary amines and the free aldehydes on the surface. Unfortunately, the formed unsaturated imines are susceptible to hydrolysis and should be reduced to more stable amine forms in an additional step. It is possible that the reduction may denature the immobilized proteins and hinder their bioactivity. Another issue with this process is that residual epoxides and grafted amines cannot be eliminated, leading to strong nonspecific adsorption and formation of unwanted covalent linkage between the surface and proteins. To overcome these problems for the case of epoxide-bearing monoliths, we developed a reaction route described in Fig. 2. In the first step of the process, the epoxide is first transformed to a 3-mercapto-2-hydroxy-propyl moiety using a phosphate-buffered sodium hydrosulfide solution (Preinerstorfer et al. 2004). The unreacted epoxide group is hydrolyzed using sulfuric acid to form a diol group which is resistant to nonspecific adsorption of antibodies or other proteins. The heterobifunctional GMBS crosslinking reagent is then grafted to the free thiol group with the maleimido terminus (Bhatia et al. 1989). The exposed and highly reactive succinmidyl ester end can then be used to capture the primary amine group on the crystallizable fragment (Fc region) of an antibody during a following immobilization reaction. Immobilization of antibody using a heterobifunctional crosslinking reagent such as GMBS is advantageous over homobifunctional dialdehyde in that the reagent does not self-couple to large reactive polymers and interfere with protein function. Furthermore, both termini of a homobifunctional crosslinking reagent may react with the functional group on the surface, decreasing the density of available reactive sites for protein immobilization. Use of heterobifunctional crosslinker can effectively solve this problem since only one end of the reagent is allowed to attach to the reactive surface. While the transformation of residual epoxide groups to diol groups by hydrolysis serves to reduce nonspecific adsorption, other nonspecific binding sites with different interaction mechanisms including electrostatic and hydrophobic interactions may still exist on the monolith surface. To reduce these interactions, the antibody-immobilized monolith was equilibrated with a 2 mg/mL BSA solution before performing an immunoassay. The relatively hydrophobic proteins adsorb on the surface to block the nonspecific binding sites while preserving the activity of immobilized antibodies.

3.3 Immunosensor characterization

Performance of the covalent antibody immobilization process was evaluated by a series of direct immunoassay tests using goat-anti rabbit IgG as a monolith-anchored antibody and FITC-labeled rabbit IgG as an antigen analyte. As an initial experiment, a solution of 50 μg/mL of antigen was infused through the monolith at a flow rate of 1 μL/min for 1 h. The same conditions were applied to a control monolith with physically adsorbed antibodies prepared using the same experimental steps including antibody introduction, but without the immobilization process shown in Fig. 2. As shown in Fig. 3, strong fluorescence saturating the CCD detector was observed in the monolith with covalently immobilized antibodies, while only a dim signal can be seen in the control immunosensor. This simple qualitative test reveals that without covalent bonding, the majority of physically adsorbed antibodies on the monolith surface were readily replaced by BSA and removed from the monolith with PBS buffer during the rinsing steps, confirming that covalent anchoring provides high antibody stability on the monolith surface.

The use of a porous monolith as an antibody support provides several significant benefits compared to a conventional flow-through immunosensor with a planar or open-tubular support. On one hand, the large surface area of the monolith facilitates efficient interactions between antigens and antibodies, and results in a high areal density of labeled antigens for increased readout sensitivity. Note also that for flow-through immunosensors, analyte residence time decreases monotonically with increasing flow rate, with a corresponding drop in the formation of antibody-antigen complexes on the sensor surface. For the case of a porous monolith, many irregular flow channels can be found within the monolith support, with average pore diameters below *ca*. 5 μm (see Fig. 1). Compared to an open-tubular support, the small pores significantly reduce the diffusion length required for antigens to reach the monolith surface, ensuring rapid formation of antibody-antigen complexes. At the same time, as sample solution is infused through the monolith, chaotic flow patterns involving both convection and diffusion are induced (Unger et al. 2008), further speeding the transport of antigens from the bulk solution to the surface. We investigated this prediction by injecting a 10 ng/mL antigen solution through a monolith immunosensor at different flow rates until the recorded fluorescence intensity was stable, then plotting the time needed to reach 90% saturated intensity (τ) against the flow rate (q) as depicted in Fig. 4. As expected, higher flow rates lead to a reduction in τ. The q-τ nonlinear relationship can be attributed to a combination of effects. While the total number of antigen molecules delivered through the monolith increases linearly with q, their characteristic diffusion length scales with $q^{-1/2}$ so that a smaller ratio of antigens reaches the monolith surface as q is increased. Note that for the range of flow rates and monolith geometry explored in this work, the characteristic IgG diffusion length is as small as 1.5 μm, well below the average pore half-width. Surface shear forces at higher flow rates may also play a role by causing dissociation of previously-formed antibody-antigen complexes.

To evaluate the concentration limit of detection (LOD) of the immunosensor, a dynamic test was used, with 10 μL volumes of antigen solutions at varying antigen concentrations continuously loaded through the monoliths at 2 μL/min for 5 min. As shown in Fig. 5, a nearly linear relation is revealed between the background corrected fluorescence intensity and antigen concentration. Substitution of 3 times of the standard deviation (SD) of the blank signal (SD_{blank} = 380), i.e. sensor background, for the intensity in the fitted linear equation (background corrected intensity = 211 × antigen concentration in ng/mL, R^2 = 0.99) yields a predicted concentration LOD of 5 ng/mL for the chosen flow rate and infusion time.

Because antigen was continuously infused through the monolith in this dynamic flow-through experiment, the concentration LOD can be pushed towards even lower limits by simply increasing the sample loading, i.e. by increasing the flow rate or infusion time. To evaluate the molar LOD of the monolith immunosensor, an alternate set of experiments were performed in which fixed 1 μL volumes of antigen solutions at different concentrations were loaded into the monolith, followed by a 10 min incubation. The resulting fluorescence intensity vs. concentration profile is shown in Fig. 6, revealing a nearly linear relationship (background corrected intensity = 0.59 ×analyte amount in amol, R^2 = 0.97) from 10 pg (~70 amol) to1000 pg (~7000 amol). The molar LOD is estimated to be 700 amol (~100 pg) using the same method employed for the determination of the concentration LOD (SD_{blank} = 138). In the measurement of samples with amounts close to the molar LOD, the fluorescence signal arising from antigen-antibody binding is indistinguishable with the intrinsic background fluorescence of the monolith.

4. Conclusions

We have developed a novel immunosensor using a surface-reactive GMA-SR454 monolith as a solid support. The porous monolith material provides a large reactive surface area for effective immobilization of capturing molecules, as well as a complex network of microscale flow paths for increased mass transport of target molecules between the bulk solution and surface-immobilized capture probes. Together with the ability to fabricate miniature monolith zones *in situ* within capillary or microchannel systems, these unique features are essential to the fabrication of immunosensors with fast response, large dynamic range and high sensitivity. A reaction process involving thiol treatment, acid hydrolysis and heterobifunctional crosslinker grafting was utilized to replace the diamine-dialdehyde grafting process commonly used in antibody immobilization, thus avoiding problems such as protein denaturing and formation of polymeric proteins. Direct immunoassays were performed to demonstrate the effectiveness of the monolith immunosensors with covalently-bound antibodies. As expected, the time required to saturate the sensors decreased with an increase in flow rate, providing a simple means for accelerating sensor response for rapid detection. Detection limits were evaluated on the basis of both concentration and molar LODs, and it was confirmed that the sensors can provide sensitivity rivaling that of traditional immunosensor platforms requiring significantly larger sample amounts and overall assay times. Although a direct immunoassay format was demonstrated in this initial work, other assay types including sandwich assays can be readily implemented with the monolith immunosensor elements. The monolith technology is also directly transferable to microfluidic platforms for the development of rapid, sensitive, multiplexed and disposable immunosensors desirable for point-of-care diagnostics and in-field environmental or forensic analysis.

Acknowledgments

This research was supported by the National Institutes of Health grant R01GM072512. SEM images were taken in Materials Research Science and Engineering Center at the University of Maryland (UMD MRSEC).

References

Abdel-Hamid I, Ivnitski D, Atanasov P, Wilkins E. Biosens. Bioelectron. 1999; 14(3):309–316. [PubMed: 10230031]

Alvarez SD, Li CP, Chiang CE, Schuller IK, Sailor MJ. ACS Nano. 2009; 3(10):3301–3307. [PubMed: 19719156]

Anderson FP, Miller WG. Clin. Chem. 1988; 34(7):1417–1421. [PubMed: 3292084]

Bae YM, Oh BK, Lee W, Lee WH, Choi JW. Anal. Chem. 2004; 76(6):1799–1803. [PubMed: 15018586]

Bakaltcheva IB, Ligler FS, Patterson CH, Shriver-Lake LC. Anal. Chim. Acta. 1999; 399(1-2):13–20.

Bangar MA, Shirale DJ, Chen W, Myung NV, Mulchandani A. Anal. Chem. 2009; 81(6):2168–2175. [PubMed: 19281260]

Bange A, Halsall HB, Heineman WR. Biosens. Bioelectron. 2005; 20(12):2488–2503. [PubMed: 15854821]

Benito-Pena E, Moreno-Bondi MC, Orellana G, Maquieira K, Van Amerongen A. J. Agric. Food Chem. 2005; 53(17):6635–6642. [PubMed: 16104778]

Bhatia SK, Shriverlake LC, Prior KJ, Georger JH, Calvert JM, Bredehorst R, Ligler FS. Anal. Biochem. 1989; 178(2):408–413. [PubMed: 2546467]

Biagini RE, Smith JP, Sammons DL, MacKenzie BA, Striley CAF, Robertson SK, Snawder JE. Anal. Bioanal. Chem. 2004; 379(3):368–374. [PubMed: 15118800]

Borisov SM, Wolfbeis OS. Optical biosensors. Chem Rev. 2008; 108(2):423–461. [PubMed: 18229952]

Charles PT, Gauger PR, Patterson CH, Kusterbeck AW. Environ. Sci. Technol. 2000; 34(21):4641–4650.

Chen GF, Svec F, Knapp DR. Lab Chip. 2008; 8(7):1198–1204. [PubMed: 18584098]

Dai Z, Yan F, Chen J, Ju HX. Anal. Chem. 2003; 75(20):5429–5434. [PubMed: 14710822]

Dong H, Li CM, Zhang YF, Cao XD, Gan Y. Lab Chip. 2007; 7(12):1752–1758. [PubMed: 18030397]

Gervais L, Delamarche E. Lab Chip. 2009; 9(23):3330–3337. [PubMed: 19904397]

Gonzalez-Martinez MA, Morais S, Puchades R, Maquieira A, Abad A, Montoya A. Anal. Chem. 1997; 69(14):2812–2818.

Guiochon G. J. Chromatogr. A. 2007; 1168(1-2):101–168. [PubMed: 17640660]

Heinze BC, Song JY, Lee CH, Najam A, Yoon JY. Sens. Actuators, B. 2009; 138(2):491–496.

Ionescu RE, Cosnier S, Herrmann S, Marks RS. Anal. Chem. 2007; 79(22):8662–8668. [PubMed: 17953450]

Ionescu RE, Gondran C, Gheber LA, Cosnier S, Marks RS. Anal. Chem. 2004; 76(22):6808–6813. [PubMed: 15538808]

Jain SR, Borowska E, Davidsson R, Tudorache M, Ponten E, Emneus J. Biosens. Bioelectron. 2004; 19(8):795–803. [PubMed: 15128098]

Kim DN, Lee Y, Koh WG. Sens. Actuators, B. 2009; 137(1):305–312.

Kim SJ, Gobi KV, Tanaka H, Shoyama Y, Miura N. Chem. Lett. 2006; 35(10):1132–1133.

Koerner T, Turck K, Brown L, Oleschuk RD. Anal. Chem. 2004; 76(21):6456–6460. [PubMed: 15516141]

Konry T, Novoa A, Cosnier S, Marks RS. Anal. Chem. 2003; 75(11):2633–2639. [PubMed: 12948130]

Konry T, Novoa A, Shemer-Avni Y, Hanuka N, Cosnier S, Lepellec A, Marks RS. Anal. Chem. 2005; 77(6):1771–1779. [PubMed: 15762584]

Kurita R, Yokota Y, Sato Y, Mizutani F, Niwa O. Anal. Chem. 2006; 78(15):5525–5531. [PubMed: 16878891]

Lepesheva GI, Azeva TN, Knyukshto VN, Chashchin VL, Usanov SA. Sens. Actuators, B. 2000; 68(1-3):27–33.

Liu JK, Chen CF, Tsao CW, Chang CC, Chu CC, Devoe DL. Anal. Chem. 2009; 81(7):2545–2554. [PubMed: 19267447]

Mallik R, Hage DS. J. Sep. Sci. 2006; 29(12):1686–1704. [PubMed: 16970180]

Mastichiadis C, Kakabakos SE, Christofidis I, Koupparis MA, Willetts C, Misiakos K. Anal. Chem. 2002; 74(23):6064–6072. [PubMed: 12498203]

Mateo C, Abian O, Fernandez-Lorente G, Pedroche J, Fernandez-Lafuente R, Guisan JM. Biotechnol. Prog. 2002; 18(3):629–634. [PubMed: 12052083]

Mateo C, Torres R, Fernandez-Lorente G, Ortiz C, Fuentes M, Hidalgo A, Lopez-Gallego F, Abian O, Palomo JM, Betancor L, Pessela BCC, Guisan JM, Fernandez-Lafuente R. Biomacromolecules. 2003; 4(3):772–777. [PubMed: 12741797]

Matsunaga T, Maeda Y, Yoshino T, Takeyama H, Takahashi M, Ginya H, Aasahina J, Tajima H. Anal. Chim. Acta. 2007; 597(2):331–339. [PubMed: 17683747]

McCormack T, OKeeffe G, MacCraith BD, OKennedy R. Sens. Actuators, B. 1997; 41(1-3):89–96.

Munge BS, Krause CE, Malhotra R, Patel V, Gutkind JS, Rusling JF. Electrochem. Commun. 2009; 11(5):1009–1012. [PubMed: 20046945]

Narang U, Anderson GP, Ligler FS, Burans J. Biosens. Bioelectron. 1997; 12(9-10):937–945. [PubMed: 9451784]

Narang U, Gauger PR, Kusterbeck AW, Ligler FS. Anal. Biochem. 1998; 255(1):13–19. [PubMed: 9448837]

Parker CO, Lanyon YH, Manning M, Arrigan DWM, Tothill IE. Anal. Chem. 2009; 81(13):5291–5298. [PubMed: 19489595]

Peterson DS, Rohr T, Svec F, Frechet JMJ. Anal. Chem. 2002; 74(16):4081–4088. [PubMed: 12199578]

Preinerstorfer B, Bicker W, Lindner W, Lammerhofer M. J. Chromatogr. A. 2004; 1044(1-2):187–199. [PubMed: 15354438]

Rohr T, Yu C, Davey MH, Svec F, Frechet JMJ. Electrophoresis. 2001; 22(18):3959–3967. [PubMed: 11700726]

Rowe CA, Scruggs SB, Feldstein MJ, Golden JP, Ligler FS. Anal. Chem. 1999; 71:433–439. [PubMed: 9949731]

Sai VVR, Mahajan S, Contractor AQ, Mukherji S. Anal. Chem. 2006; 78(24):8368–8373. [PubMed: 17165829]

Svec F. J. Sep. Sci. 2004; 27(10-11):747–766. [PubMed: 15354553]

Svec F, Huber CG. Anal. Chem. 2006; 78(7):2100–2107.

Szekacs A, Trummer N, Adanyi N, Varadi M, Szendro I. Anal. Chim. Acta. 2003; 487(1):31–42.

Tang L, Zeng GM, Shen GL, Li YP, Zhang Y, Huang DL. Environ. Sci. Technol. 2008; 42(4):1207–1212. [PubMed: 18351094]

Unger KK, Skudas R, Schulte MM. J. Chromatogr. A. 2008; 1184(1-2):393–415. [PubMed: 18177658]

Valera E, Ramon-Azcon J, Rodriguez A, Castaner LM, Sanchez FJ, Marco MP. Sens. Actuators, B. 2007; 125(2):526–537.

Van Bergen SK, Bakaltcheva IB, Lundgren JS, Shriver-Lake LC. Environ. Sci. Technol. 2000; 34(4):704–708.

Wang RH, Ruan CM, Kanayeva D, Lassiter K, Li YB. Nano Lett. 2008; 8(9):2625–2631. [PubMed: 18715043]

Yang LJ, Li YB, Erf GF. Anal. Chem. 2004; 76(4):1107–1113. [PubMed: 14961745]

Yu C, Davey MH, Svec F, Frechet JMJ. Anal. Chem. 2001; 73(21):5088–5096. [PubMed: 11721904]

Yu X, Munge B, Patel V, Jensen G, Bhirde A, Gong JD, Kim SN, Gillespie J, Gutkind JS, Papadimitrakopoulos F, Rusling JF. J. Am. Chem. Soc. 2006; 128(34):11199–11205. [PubMed: 16925438]

Zuo BL, Li SM, Guo Z, Zhang JF, Chen CZ. Anal. Chem. 2004; 76(13):3536–3540. [PubMed: 15228322]

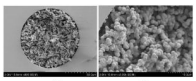

Fig. 1.
(a) Far field and (b) close up electron micrographs of a GMA-SR454 monolith.

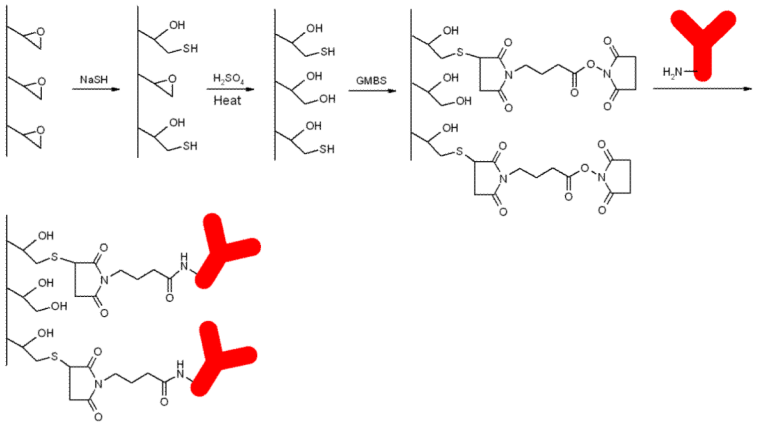

Fig. 2.

Immobilization of antibodies on GMA-SR454 monolith surface. Thiol groups are introduced by attacking epoxide groups with NaSH, and residual epoxide groups are eliminated in the following acid hydrolysis. GMBS spacer is then grafted to the thiolated monolith, enabling antibody capture through the reaction of succinimidyl ester functionality in GMBS with primary amine of antibodies.

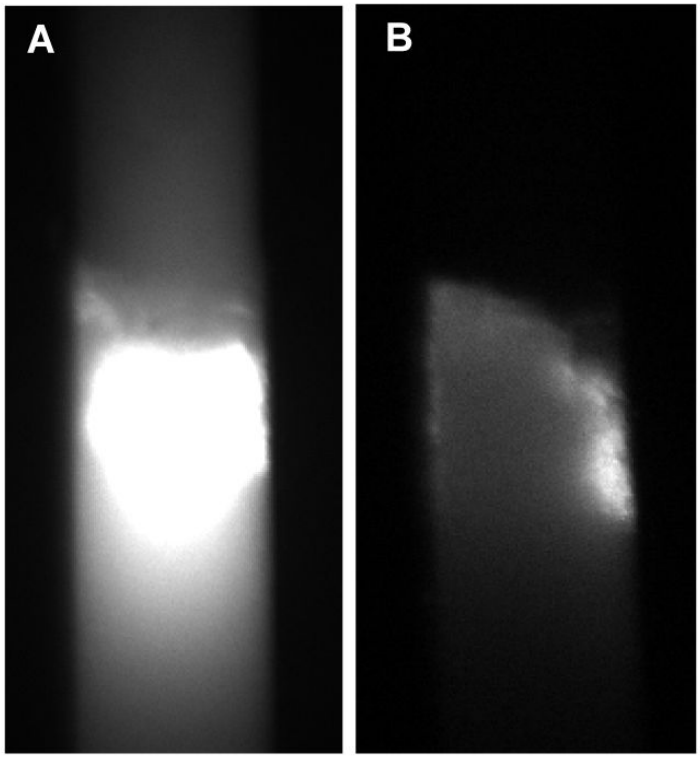

Fig. 3.
Fig.3 Direct immunoassay using monolith immunosensors with (A) covalently attached and (B) physically adsorbed antibodies.

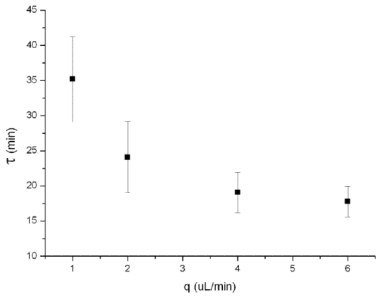

Fig. 4.

Impact of flow rate (q) to the time required to reach 90% of saturated fluorescence intensity (τ). The concentration of the FITC-antigen is 10 ng/mL. Each datum represents the average of 3 measurements.

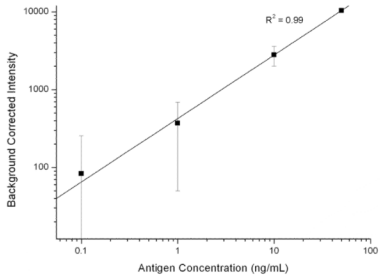

Fig. 5.

Dilution study using FITC-labeled rabbit IgG as an antigen to monolith-immobilized anti-rabbit IgG. A concentration LOD of 5 ng/mL is calculated.

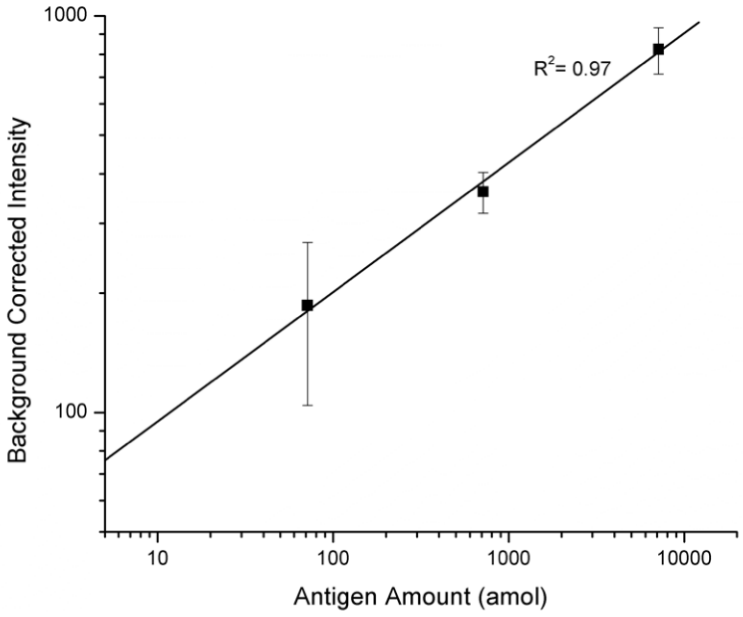

Fig. 6.

Fluorescence intensities for different FITC-labeled rabbit IgG loading amounts, defined by injecting 1μL sample volumes through the monolith elements at varying antigen concentrations, enabling the determination of molar LOD.